

FIBER BRAGG GRATING SENSOR APPLICATIONS FOR STRUCTURAL HEALTH MONITORING

CANSU KARATAŞ

*Turkish Aerospace Industries, Fethiye Mahallesi, Havacılık Bulvarı No: 17,
Ankara, 06980/Kahramankazan, Turkey
cansu.karatas@tai.com.tr*

*Aerospace Engineering, Middle East Technical University, Üniversiteler Mahallesi, Dumlupınar Bulvarı No: 1,
Ankara, 06800/Çankaya, Turkey
cansu.karatas@metu.edu.tr*

BORAY DEĞERLİYURT

*Aerospace Engineering, Middle East Technical University, Üniversiteler Mahallesi, Dumlupınar Bulvarı No: 1,
Ankara, 06800/Çankaya, Turkey
boray.degerliyurt@metu.edu.tr*

YAVUZ YAMAN

*Aerospace Engineering, Middle East Technical University, Üniversiteler Mahallesi, Dumlupınar Bulvarı No: 1,
Ankara, 06800/Çankaya, Turkey
yyaman@metu.edu.tr*

MELİN ŞAHİN

*Aerospace Engineering, Middle East Technical University, Üniversiteler Mahallesi, Dumlupınar Bulvarı No: 1,
Ankara, 06800/Çankaya, Turkey
msahin@metu.edu.tr*

Abstract

Structural Health Monitoring is defined as detecting and interpreting of the changes in the features of the structure concerned. The opportunity to avoid catastrophic failures by detecting damages in advance and also to reduce maintenance costs and labors have made the subject appealing especially for the civil engineering and aeronautical engineering fields. The systems designed for Structural Health Monitoring require sensors to collect response of the structure to the excitations which may be environmental or pre-determined. Fiber Bragg Grating sensors are denoted as one of the most promising sensors for Structural Health Monitoring applications since they are lightweight, stable and immune to electromagnetic effects. Most importantly, the ability to embed Fiber Bragg Grating sensors between the composite layers make them the ideal sensors for monitoring the health of the aerospace structures such as beams, wings, wind turbine bases, wind turbine blades and helicopter blades. In this study, Fiber Bragg Grating sensors applications and proceedings for Structural Health Monitoring of thin composite beams are presented. The system developed and utilized, including working principle of the Fiber Bragg Grating sensors, interrogator system and manufacturing of the beams equipped with embedded and surface mounted sensors, are explained. Tension and torsion tests of the composite beams are conducted to verify the effectiveness of the system which then will be adopted to compare the response of the healthy and damaged beams as a future work. In addition, comparison between the Fiber Bragg Grating sensors and conventional strain gauges is made in terms of noise by using both sensors during the tensile tests.

Keywords Structural Health Monitoring; Fiber Bragg Grating sensors; composite beams.

1. Introduction

Structural Health Monitoring (SHM) is defined by Speckman and Roesner (2006) as continuous monitoring of the structures with embedded or mounted sensors with minimum human intervention to observe the structural integrity. The ability to detect damages before failure, reduced number of maintenance cycles, shortened downtime and reduced maintenance labor are among the advantages of Structural Health Monitoring which make the subject appealing in civil, aeronautical and mechanical engineering (Boller, 2009).

SHM requires sensors to collect the response of the structures to the excitations. Then, features which indicate the condition of the structures, such as natural frequency, strain mode shape and strain, are extracted from the data

collected with the help of sensors. Finally, damage detection methods are applied on the features to investigate the health of the structure concerned. Accelerometers, strain gauges, piezoelectric sensors and fiber optic sensors are among the sensors that are commonly used for SHM applications.

Fiber Bragg Grating (FBG) sensors are fiber optic sensors based on the reflection of light with a precise wavelength called Bragg wavelength. The inherit properties of FBG sensors, such as chemical and physical compatibility, lightweight, ability to withstand harsh environment, immunity to electromagnetic interference and ability to be embedded between the layers of composite structures, make them advantageous to utilize for SHM applications on composite structures (Takeda *et al.*, 2002; Costa *et al.*, 2014).

In this study, static tests of composite beams with embedded and surface mounted FBG sensors under tension and torsion loads are conducted to observe the suitability of the FBG sensors for SHM applications on composite structures. Results obtained from the tests and the Finite Element Analyses (FEA) are compared to observe the agreement between them. In addition, axial strain results obtained from a FBG sensor and a strain gauge on the surface of a composite beam are compared to monitor and compare the noise in data.

2. The Fiber Bragg Grating Sensor System Utilized Throughout the Study

In this section, the properties of FBG sensors and interrogator system utilized for the current study will be explained.

2.1. Fiber Bragg Grating sensors

FBG sensors are produced by interfering part of a photosensitive fiber optic cable with UV laser beam so as to change the refractive index of the interfered part, as demonstrated in Figure 1 (Smart Fibres, 2017a). FBG sensors reflect a narrowband light beam called Bragg wavelength when exposed to a broadband laser beam. Working principle of FBG sensors is based on shift in the Bragg wavelength due to elongation or retraction. Then, algorithms are used to transform the shift in the Bragg wavelength to strain data.

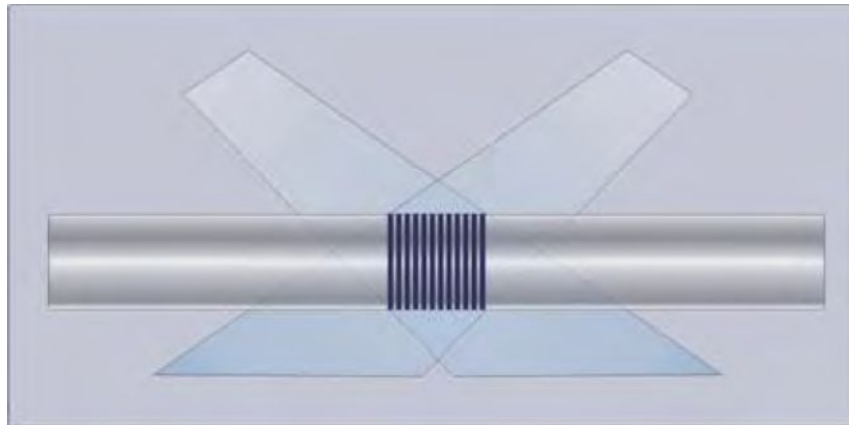


Figure 1. FBG Sensor Produced by Interference of UV Laser Beams (Smart Fibres, 2017a)

The optical strain sensors utilized for the current study are single FBG sensors recorded on Single Mode fiber optic cables, produced by Smart Fibres. Polyimide coating, which allows applications in a temperature range of -270°C to $+300^{\circ}\text{C}$, is preferred such that the sensors could withstand the high temperatures during the curing process of the composites. FBG sensors are available in lengths of 1 mm, 2 mm, 5 mm and 10 mm. The strain range is between $-9000\ \mu\text{strain}$ and $+9000\ \mu\text{strain}$ (Smart Fibres, 2017a). Fiber optic cables, on which the FBG sensors are recorded, are connected to the interrogator system with the help of pigtail connectors. FBG sensor, fiber optic cable and pigtail connectors are presented in Figure 2 (Karataş, 2017).

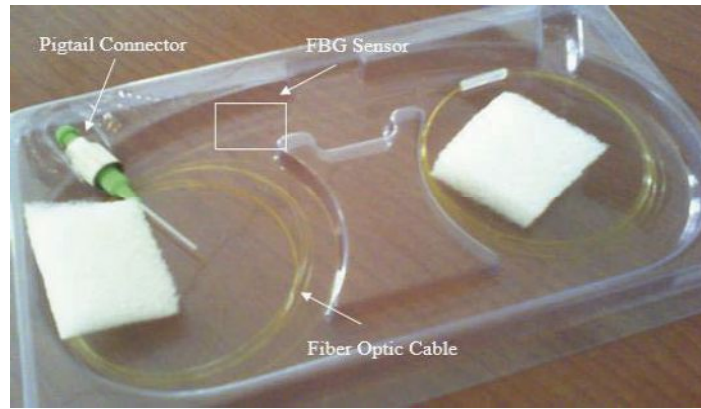


Figure 2. FBG Sensor on Fiber Optic Cable with Pigtail Connector (Karataş, 2017)

2.2. Interrogator system

Interrogator is a device which beams laser light into the fiber optic cable and measures the change in the Bragg wavelength of a FBG sensor. Then, interrogator transforms the wavelength data into strain. Interrogator system used for the current study is SmartScan Aero Interrogator produced by Smart Fibres for high frequency and harsh environment applications, as presented in Figure 3. The device has four optical channels through which 16 sensors per channel could be interrogated. Maximum scanning frequency is stated as 25 kHz, if single FBG sensor is connected, and as 2.5 kHz, if all the 64 sensors are simultaneously connected. The interrogator could log data for 24 hours, generating 16 GB of data (Smart Fibres, 2017b). The data is collected by connecting the interrogator to a computer which has the SmartSoft software installed.



Figure 3. SmartScan Aero Interrogator (Smart Fibres, 2017b)

3. Manufacturing Composite Beams with Embedded and Surface Bonded Fiber Bragg Grating Sensors

Composite beams are manufactured from glass-epoxy prepreg composite materials with the layup sequence $[0_g/\text{Film}/(\pm 45)_{\text{Woven}}]_s$. The layers for each beam are cut separately in their exact dimensions with the help of an industrial cutting machine such that finishing operations are performed conveniently. Layup is continued until the layer on which the FBG sensor will be placed is reached. Then, the FBG sensors are positioned on the composite layer in longitudinal direction for the tension tests and in angular direction ($\pm 45^\circ$ from the longitudinal direction) for the torsion tests, as presented in Figure 4 and in Figure 5. Also, as seen in Figure 4 and Figure 5, fiber optic cables are covered with Teflon tubes at the egress regions to ensure the health of the cables. Then, layup is continued for the remaining layers. Finally, the beams are cured in autoclave simultaneously to eliminate the effects that might be caused by the differences in curing conditions. An important detail is that composite beams manufactured for the tension tests have tabs secondarily bonded to the ends of them.

The wavelength of the FBG sensors are checked before and after embedment, vacuuming and curing processes. In addition, the pigtail connectors are cut from the fiber optic cables since they are expected to melt during the curing process. The pigtail connectors will be connected to the fiber optic cables using splicer device after the curing process is completed.

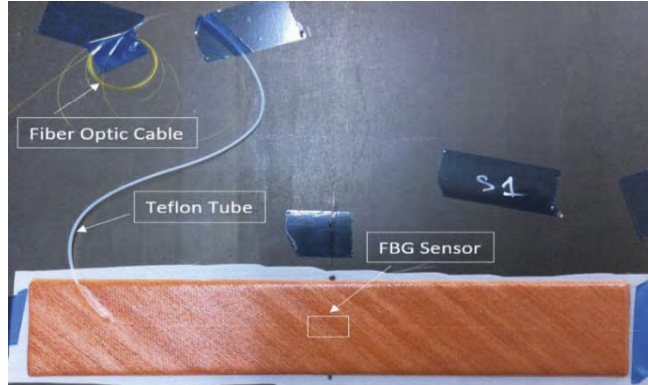


Figure 4. Embedment of FBG Sensor into the Composite Beam for the Tension Tests

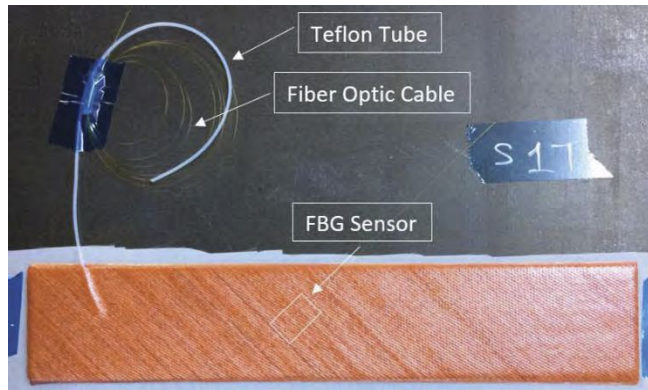


Figure 5. Embedment of FBG Sensor into the Composite Beam for the Torsion Tests

All the manufactured composite beams along with the positions of the FBG sensors and strain gauges on them could be found in Table 1.

Table 1. FBG Sensor and Strain Gauge Positions of Composite Beams

	The Beam	FBG	Position		
			Longitudinal	Transverse	Thickness
The Beams for Tension Test	S1	FBG1	Middle	Middle	Surface
		FBG2	Middle	Middle	Embedded between Woven Layers
	S2	FBG1	Middle	Middle	Surface
		FBG2	Middle	Middle	Embedded between UD Layers
	S3	FBG1	Middle	Middle	Surface
		SG	Middle	Middle	Surface
The Beams for Torsion Tests	S1T	FBG1	Middle	Middle	Surface
		FBG2	Middle	Edge	Embedded between Woven Layers
	S2T	FBG1	Middle	Middle	Surface
		FBG2	Middle	Middle	Embedded between UD Layers
		FBG3	Middle	Edge	Embedded between Woven Layers
	S3T	FBG1	Middle	Middle	Surface
FBG2		Middle	Middle	Surface	

4. Static Tests of Composite Beams under Tension and Torsion Loads

6.1. Procedure for the static tests under tension load

MTS Axial Test System is used to apply static tension load to the composite beams. One end of the beams is fixed in all directions, and the other end is only applied an axial displacement of 2 mm. Axial force and displacements are measured with the load cell on the test system, whereas axial strains are measured with the FBG sensors. Figure 6 presents one of the composite beams mounted to the test machine and FBG sensors connected to the interrogator system.

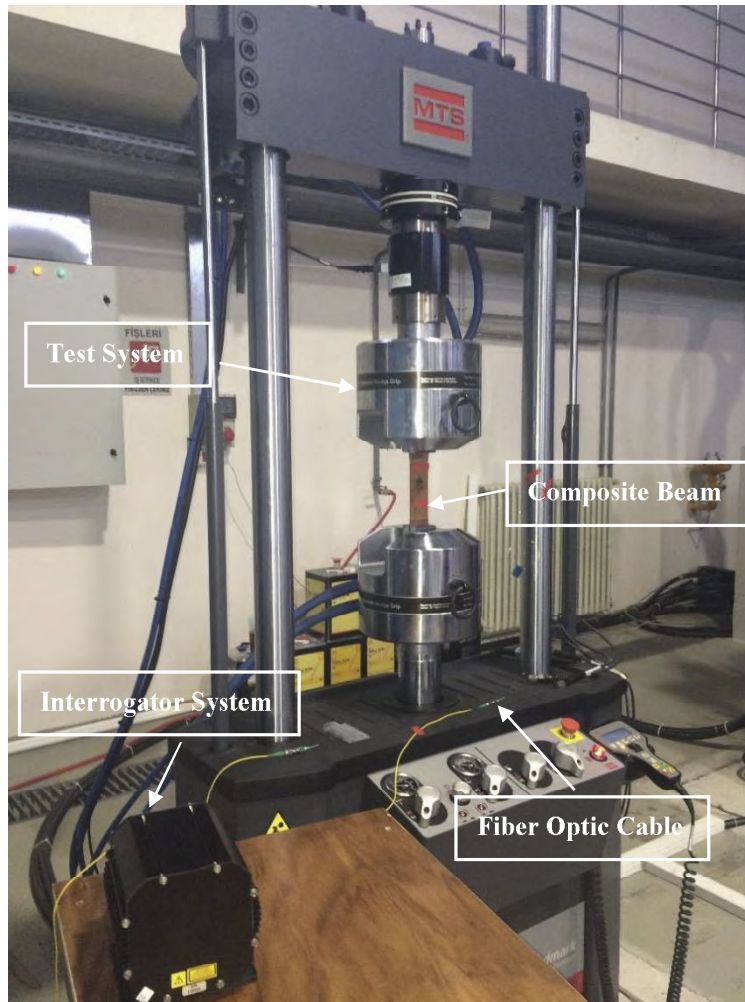


Figure 6. Composite Beam with Embedded FBG Sensors Mounted to the MTS Axial Test System

4.2. Procedure for the static tests under torsion load

MTS 809 Axial/Torsional Test System, which could apply tension and torsion loads at the same time, is used for static tests under torsion load. All the composite beams are applied torsional load corresponding to a 20° of angle of twist. One end of the beams is fixed in all directions. However, the other end is allowed to move in longitudinal direction using force control, and around axial direction using displacement control. Composite beams with embedded FBG sensors are mounted to the test machine very carefully for not to damage the fragile fiber optic cables. Torque, axial force and axial displacement are collected from the test system, whereas shear strain is collected from the FBG sensors. Each beam is tested three times for the same angle of twist to observe repeatability. Figure 7 presents one of the composite beams twisted to 20° of angle of twist.



Figure 7. Composite Beam with Embedded FBG Sensors Mounted to the MTS 809 Axial/Torsional Test System

5. Finite Element Analysis of Composite Beams under Tension and Torsion Loads

Finite Element Analysis of composite beams are performed for tension and torsion tests using the commercial finite element code ABAQUS®. The results obtained from the FEA will be compared with the ones obtained from the static tests.

Composite layers are modeled as orthotropic materials. It is convenient to model the same layers as one layer. In addition, only linear elastic material properties of composite layers are input to the ABAQUS® for the FEA.

Finite elements are C3D8R elements which are solid, 8-node, linear elements with reduced integration. Isometric view of the mesh structure of the beams for tension load is presented in Figure 8. Only a quarter of the beams is modeled for the tension load. In addition, Figure 9 presents isometric view and cross-sectional view of the mesh structure of the beams for torsion load. Observe that the mesh structure of the FEM for torsion load is finer than the one for tension load.

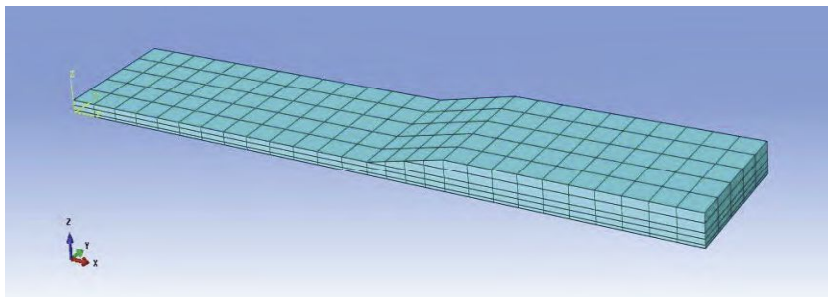


Figure 8. Mesh Structure of Composite Beams for Tension Load

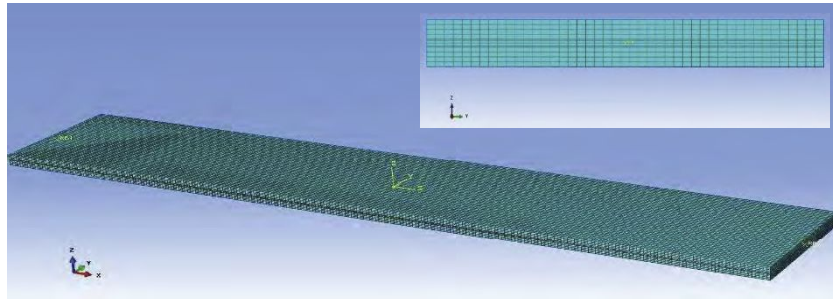


Figure 9. Mesh Structure of Composite Beams for Torsion Load

6. Results Obtained from the Tests and Finite Element Analyses

The results obtained from the tests and FEA are compared in this section separately for the static tests under tension load and under torsion load. All the results presented in this study are based on the thesis studies of authors (Değerliyurt, 2017; Karataş, 2017).

6.1. Results obtained from the static tests under tension load and Finite Element Analyses

Axial force – axial strain curves gathered from the FBG sensors on the surface of each beam including all the tests are presented in Figure 10, which signifies that the repeatability of the tests is accomplished.

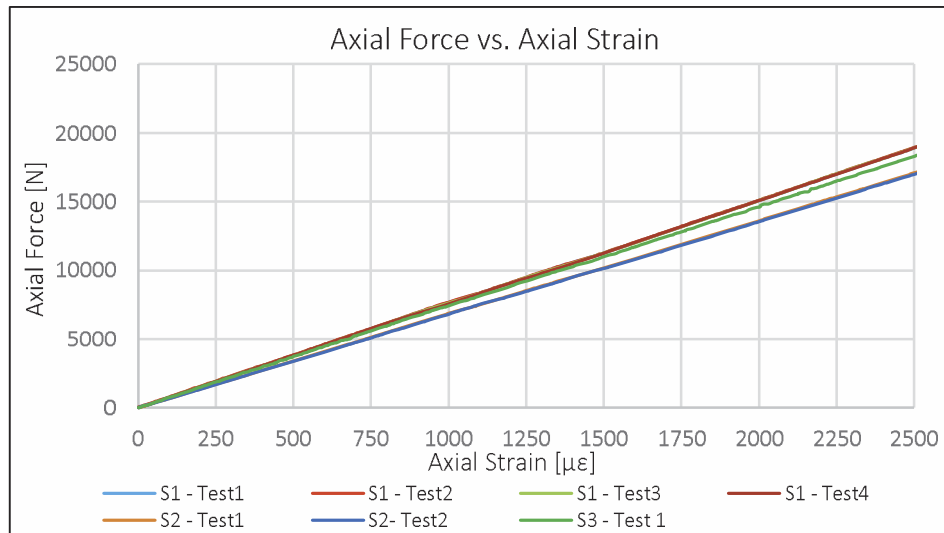


Figure 10. Axial Force – Axial Strain Curves for Composite Beams under Tension Load

Axial force – axial strain curves gathered from the average results of the tests of all the beams and from the FEA are compared in Figure 11. Axial strain results obtained from all the sensors should be the same in the same cross section. It is observed that embedded and surface bonded FBG sensors give the same results, as expected. In addition, FEM results are very close to the test results. The small difference between the results might be caused by the errors in alignment of the sensors.

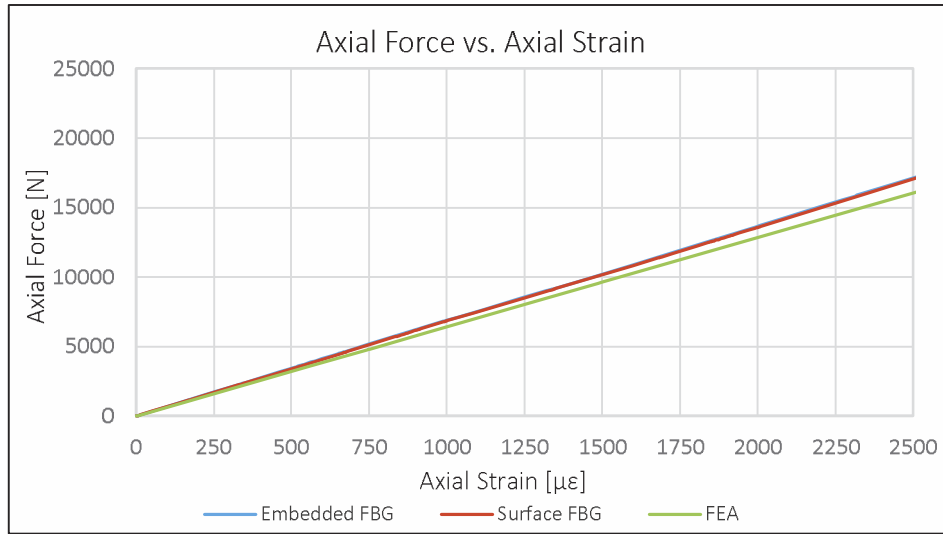


Figure 11. Axial Force – Axial Strain Curves Obtained from the Tests and FEA

6.2. Results obtained from the static tests under torsion load and Finite Element Analyses

There are both negative and positive values of angle of twist, torque and shear strain results presented in this section. Axes of the graphs are arranged such that the comparison of the data becomes easier.

Torque – angle of twist curves of each beam from all three tests are presented in Figure 12, which indicates that the repeatability of the tests is achieved.

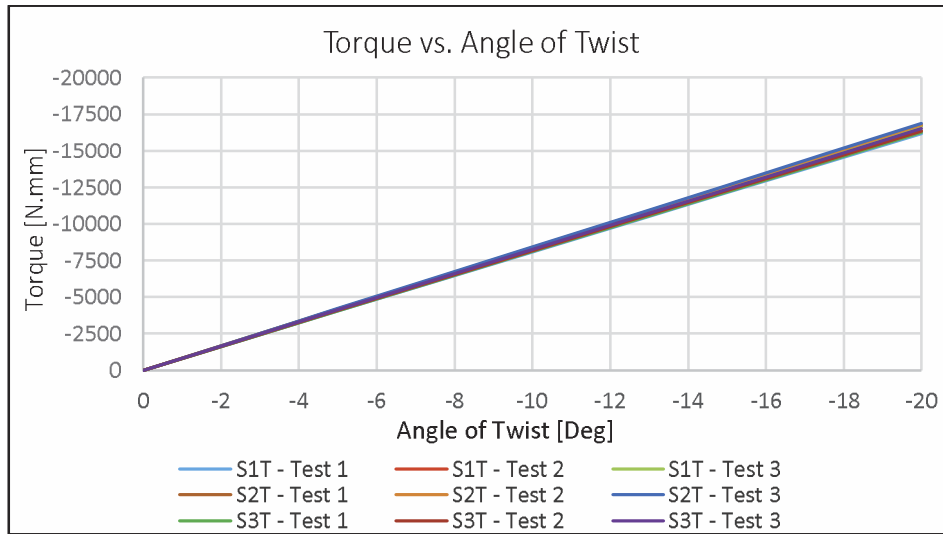


Figure 12. Torque - Angle of Twist Curves for Composite Beams under Torsion Load

The torque - angle of twist and shear strain – angle of twist results gathered from the averages of the three tests of all the beams and from the FEA are compared in Figure 13 – Figure 17. As expected, the shear strain value increases with increasing distance from the middle plane. In addition, it is observed that the results gathered from the tests and FEA are sufficiently close to each other; however, there is a little difference between the results which increases with increasing angle of twist. The reason behind this behavior could be the fact that material nonlinearity is not included in the FEA. Also, errors in alignment of the sensors could affect the results.

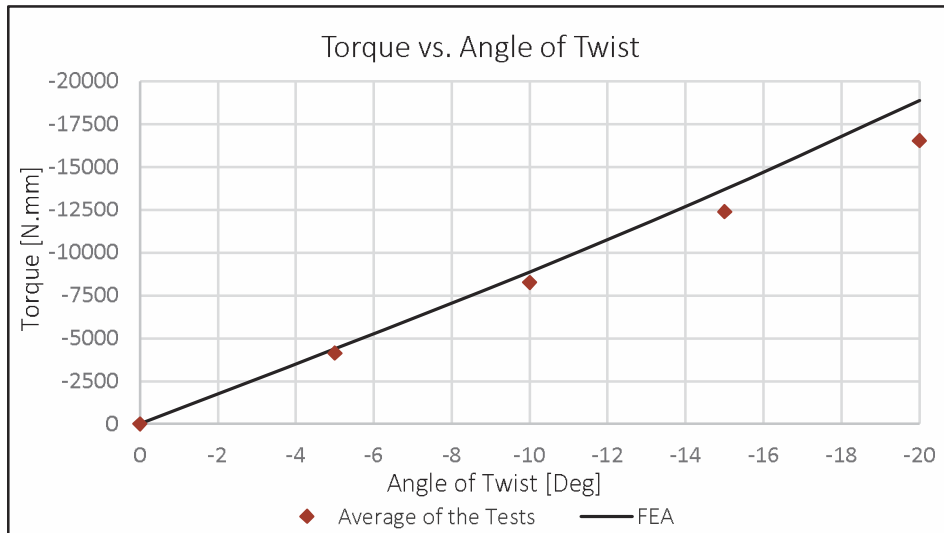


Figure 13. Torque – Angle of Twist Curves Obtained from the Tests and FEA

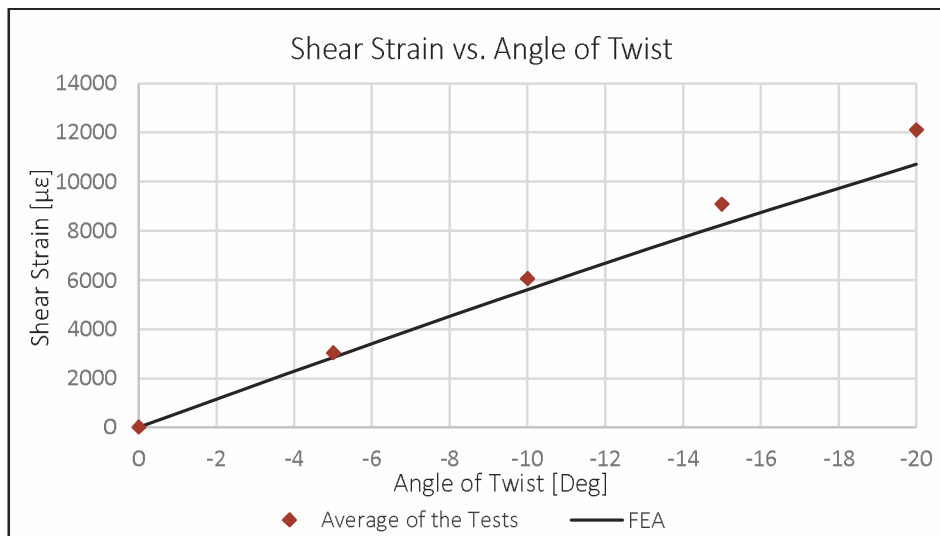


Figure 14. Shear Strain (Positive) – Angle of Twist Curves Obtained from the FBG Sensors on the Surface of the Beams and from the FEA

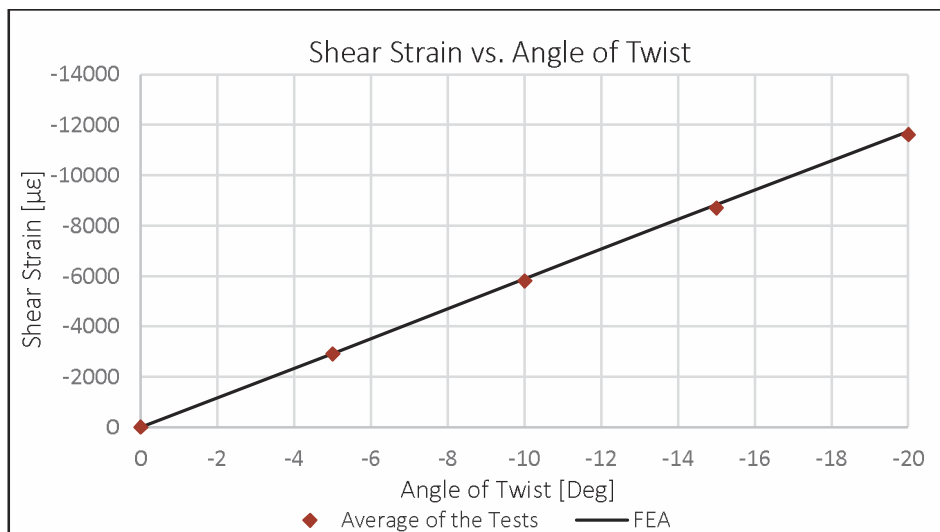


Figure 15. Shear Strain (Negative) – Angle of Twist Curves Obtained from the FBG Sensors on the Surface of the Beams and from the FEA

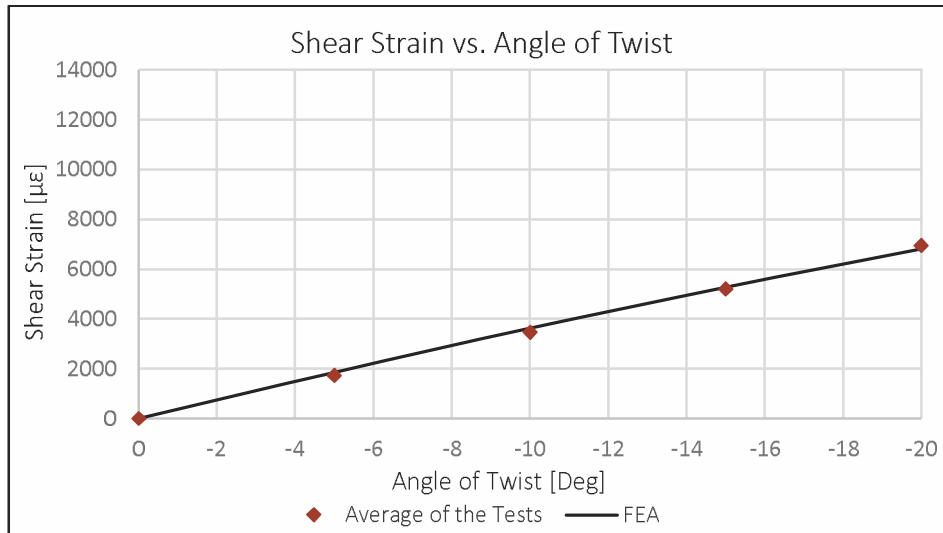


Figure 16. Shear Strain – Angle of Twist Curves Obtained from the FBG Sensors Embedded between the UD Layers and from the FEA

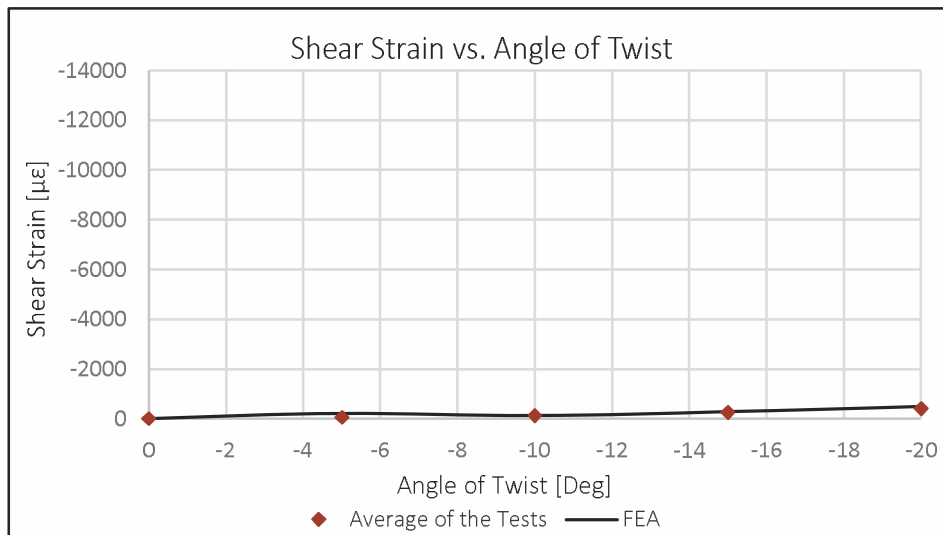


Figure 17. Shear Strain – Angle of Twist Curves Obtained from the FBG Sensors Embedded between the Woven Layers and from the FEA

7. Tension Test of Composite Beam Equipped with Both FBG Sensor and Strain Gauge

A case study to compare the strain results collected from the FBG sensors and strain gauges is conducted as a part of the study. The beam S3 has one FBG sensor bonded on its surface and one strain gauge bonded on its other surface. It is observed that the axial strain results obtained from static tensile test of S3 coincide, as seen in Figure 18. In addition, the noise in data gathered from both sensors is investigated, with the conclusion that the data collected using the FBG sensors is less noisy compared to the one collected using the strain gauges, as presented in Figure 19.

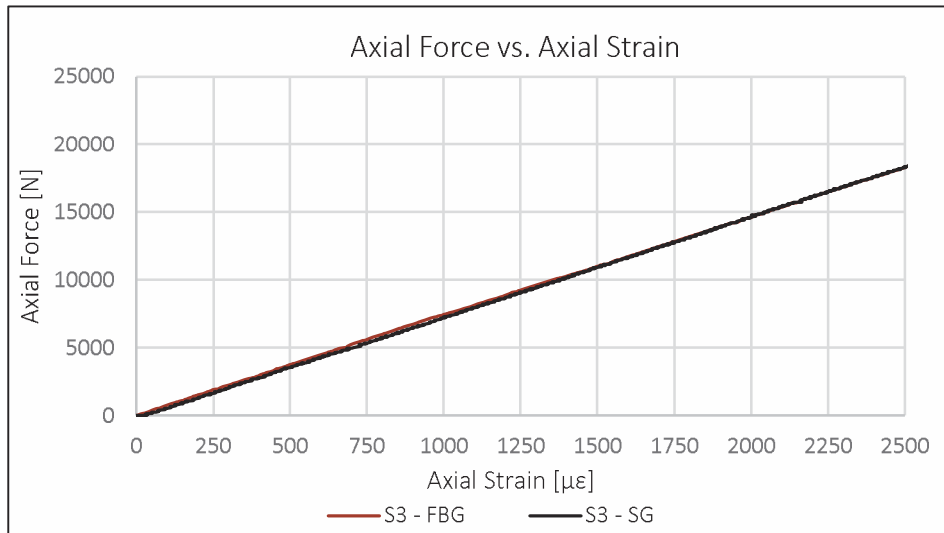


Figure 18. Axial Force – Axial Strain Curves Obtained from the FBG Sensor and Strain Gauge on the Surface of S3

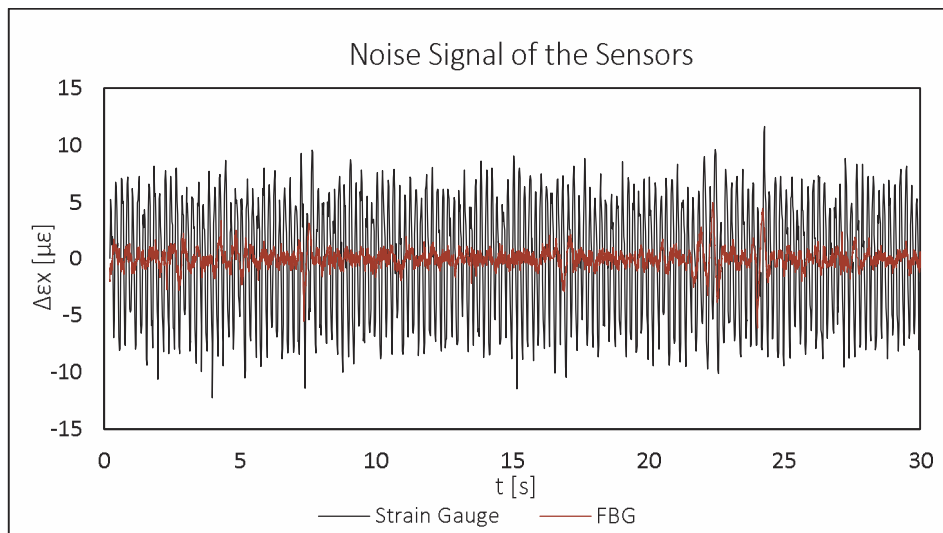


Figure 19. Noise Signal of the Axial Strain Data Obtained from the FBG Sensor and Strain Gauge on the Surface of S3

8. Conclusion

In this study, static tension and torsion test results of composite beams equipped with embedded and surface bonded FBG sensors are presented. Repeatability of the tests is achieved by repeating the tests under the same conditions. Also, it is observed that the results obtained from the tests and FEA are close to each other. The difference increasing with increasing angle of twist might be caused by not including the material nonlinearity in the FEA. In addition, it is presented that axial force – axial strain curves obtained from a FBG sensor and a strain gauge bonded to the two surface of a composite beam coincide. Finally, the noise in the axial strain data is compared for both sensors. It is demonstrated that the data collected from the strain gauge is noisy than the one from the FBG sensor. Considering the issues mentioned before, it could be said that FBG sensors are able and feasible for SHM applications on composite structures.

9. Future Work

Fatigue tests of composite beams with embedded and surface bonded FBG sensors could be performed to observe the durability of the FBG sensors. In addition, fatigue tests of intentionally damaged composite structures might

be conducted to examine whether it is able to detect damage propagation using the strain data obtained by the embedded FBG sensors. The damage might be induced to the structures by thin Teflon plates.

Acknowledgements

This study is financed by Turkish Aerospace Industries as a part of the project conducted for Rotary Wing Technology Center.

References

- Boller C. (2009). Structural Health Monitoring – An Introduction and Definitions. *Encyclopedia of Structural Health Monitoring*. John Wiley and Sons, Inc.
- Costa J. M. *et al.* (2014). Fiber-optically sensorized composite wing. *SPIE Smart Structures and Materials+ Nondestructive Evaluation and Health Monitoring*, **9062**: 906213 1-6. International Society for Optics and Photonics.
- Değerliyurt B. (2017). Development and Experimental Verification of a Structural Health Monitoring System for Composite Beams with Embedded Fibre Bragg Grating Sensors. M.S. Thesis. Middle East Technical University, Ankara, Turkey.
- Karataş C. (2017). Finite Element Analysis and Tests of Composite Beams with Fiber Bragg Grating Sensors under Torsional Load for Structural Health Monitoring Applications. M.S. Thesis. Middle East Technical University, Ankara, Turkey.
- Smart Fibres Ltd, UK (2017a). SmartFBG Fibre Bragg Grating Sensor Technical Data Sheet.
- Smart Fibres Ltd, UK (2017b). SmartScan Aero Interrogator Technical Data Sheet.
- Speckmann H. and Roesner H. (2006). Structural Health Monitoring: A Contribution to the Intelligent Aircraft Structure. *Proceedings of the 9th European Conference on NDT (ECNDT), Berlin, Germany*, **2529**.
- Takeda S. and Okabe Y., Takeda N. (2002). Delamination Detection in CFRP Laminates with Embedded Small-diameter Fiber Bragg Grating Sensors. *Composites Part A: applied science and manufacturing*, **33.7**: 971-980.